Detection of molecular interactions at membrane surfaces through colloid phase transitions

Michael M. Baksh[1,2], **Michal Jaros**[1] **& Jay T. Groves**[1,2]

[1]*Department of Chemistry, University of California and* [2]*Physical Bioscience Division, Lawrence Berkeley National Laboratory, Berkeley, California 94720, USA*

The molecular architecture of—and biochemical processes within—cell membranes play important roles in all living organisms, with many drugs and infectious disease agents targeting membranes. Experimental studies of biochemical reactions on membrane surfaces are challenging, as they require a membrane environment that is fluid (like cell membranes) but nevertheless allows for the efficient detection and characterization of molecular interactions. One approach uses lipid membranes supported on solid substrates such as silica or polymers[1,2]: although the membrane is trapped near the solid interface, it retains natural fluidity and biological functionality[3] and can be implanted with membrane proteins for functional studies[4]. But the detection of molecular interactions involving membrane-bound species generally requires elaborate techniques, such as surface plasmon resonance [5] or total internal reflection fluorescence microscopy[6]. Here we demonstrate that colloidal phase transitions of membrane-coated silica beads provide a simple and label-free method for monitoring molecular interactions on lipid membrane surfaces. By adjusting the lipid membrane composition and hence the pair interaction potential between the membrane-supporting silica beads, we poise our system near a phase transition so that small perturbations on the membrane surface induce dramatic changes in the macroscopic organization of the colloid. We expect that this approach, used here to probe with high sensitivity protein binding events at membrane surfaces, can be applied to study a broad range of cell membrane processes.

Colloidal particles self-assemble into a variety of ordered phases, and the study of colloidal phase transitions is currently an area of intensive activity [7]. This collective effort is fuelled by the intriguing statistical thermodynamic behaviour of colloids, their general applicability to the study of phase transitions, and their important material properties, such as the ability to self assemble into ordered structures[8–12]. The behaviour of a colloidal system is driven by the pair interaction potential between particles. In the case of membrane-derivatized silica beads, the pair potential is dominated by membrane–membrane interactions. Two-dimensional dispersions of lipid-membrane-derivatized silica beads exhibit colloidal phase transitions that are governed by details of these membrane surface interactions. The collective phase behaviour serves as a cooperative amplifier that produces a readily detectable response from a small number of molecular events on the membrane surface. Using direct optical imaging, we observe multiple near-equilibrium phases and find that protein binding to membrane-associated ligands at densities as low as 10^{-4} monolayer can trigger a phase transition. Statistical analysis of bead pair distribution functions enables quantitative comparison among different membrane systems and reveals subtle, pre-transition effects.

Lipid membranes can be assembled on silica beads by essentially the same vesicle fusion process used to form supported membranes on monolithic substrates[13,14]. The resulting membrane, illustrated schematically in Fig. 1a, is continuous and retains lateral fluidity. Figure 1b and c depicts fluorescence recovery after photobleaching (FRAP) experiments performed on beads coated with fluid and

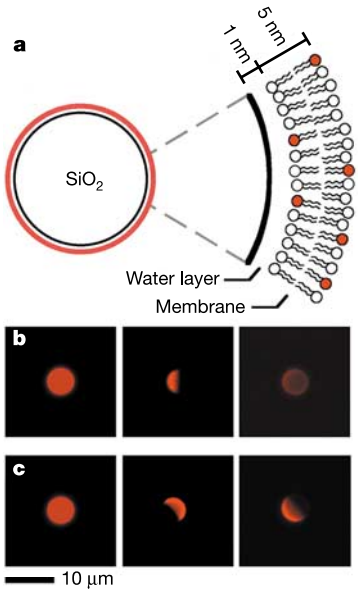

Figure 1 Membrane-derivatized bead. **a**, Schematic illustration of a membrane-derivatized silica bead. **b**,**c**, FRAP experiments conducted on beads coated with fluid (**b**; 88% 1,2-dimyristoleoyl-*sn*-glycero-3-phosphocholine (DMOPC), 11% 1,2-dioleoyl-*sn*-glycero-3-ethylphosphocholine (DOEPC), 1% *N*-(Texas red sulphonyl)–1,2-dipalmitoyl-*sn*-glycero-3-phosphoethanolamine (Texas red–DPPE) fluorescent probe) and non-fluid (**c**; 88% 1,2-dipalmitoyl-*sn*-glycero-3-phosphocholine (DPPC), 11% DOEPC, 1% Texas red–DPPE) lipid membranes. Full illumination before bleach (left panel), exposure pattern during bleach (middle panel), full illumination 1 min after bleach (right panel).

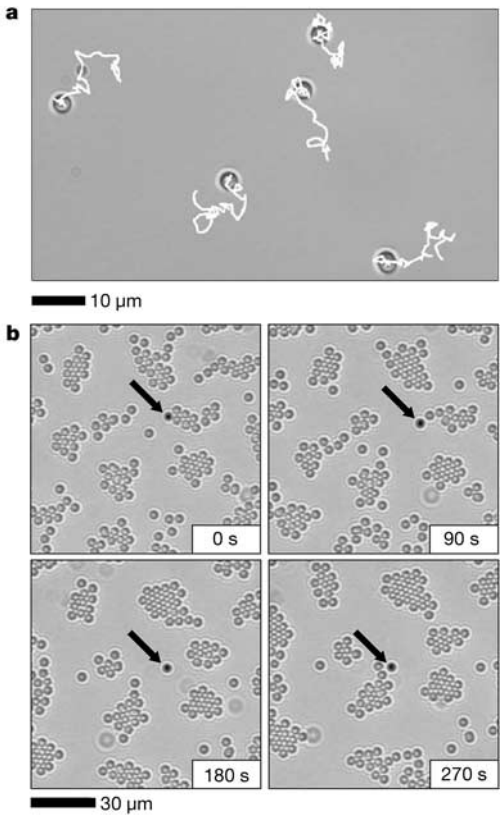

Figure 2 Mobility of membrane-derivatized beads. **a**, Two-dimensional brownian trajectories of membrane-derivatized beads, which have settled gravitationally to the bottom of a dish filled with water. Diffusion coefficients are independent of membrane composition, and ranged from 0.079 to 0.086 $\mu m^2 s^{-1}$ for 5-μm-diameter beads. **b**, Time sequence images of a condensed phase of the colloid, illustrating the mobility of individual beads into and out of condensed crystallites. The arrow identifies the moving position of an individual bead through the four frames.

non-fluid (gel state) membranes, respectively. Diffusion coefficients of 1–5 $\mu m^2 s^{-1}$, as seen here, are typical of fluid membranes. Silica beads can be derivatized with membranes varying widely in composition, providing a precise method of adjusting the chemical and biological constitution of the surface.

Membrane-derivatized silica beads were dispersed, underwater, where they settle gravitationally onto the underlying substrate and form a two-dimensional colloid. The beads exhibit free lateral diffusion, and the system behaves as an ergodic fluid. Brownian trajectories for a dilute collection of beads are illustrated in Fig. 2a. Bead diffusion coefficients are essentially independent of membrane composition; measurements ranged from 0.079 to 0.086 $\mu m^2 s^{-1}$ for 5-μm-diameter beads. These values are ~80% of that predicted by the Stokes–Einstein relation for purely viscous drag, indicating a small contribution from drag on the underlying substrate. Depending on the strength of the interaction between membranes on the bead surfaces, dispersed (gas) or condensed (liquid or crystalline) phases of the colloid are observed. Bead mobility is retained in condensed phases (Fig. 2b). The mobility of individual beads, in both condensed and dispersed phases, defines the rate of system equilibration. The timescale of bead condensation onto and evaporation from the condensed crystallites, seen in Fig. 2b, is rapid compared to that of our experiments (several minutes versus more than half an hour). Additionally, the overall morphology and quantitative pair distribution functions of the phases remain constant, despite the interchange of individual beads. These observations suggest that the system is near equilibrium, at least over length scales of several bead diameters.

The chemical composition of the lipid membrane was adjusted to modulate the pair interaction potential. Condensed phases, as seen in Fig. 2b, formed whenever the coating membrane was net neutral or negatively charged. In contrast, net positively charged membranes led to dispersed phases. The occurrence of multiple phases indicates that pair interaction energies place the system near a phase transition. As such, small perturbations on the membrane surface are expected to induce significant changes in the macroscopic organization of the colloid. We observe this predicted behaviour when examining the effects of protein binding to membrane-associated ligands.

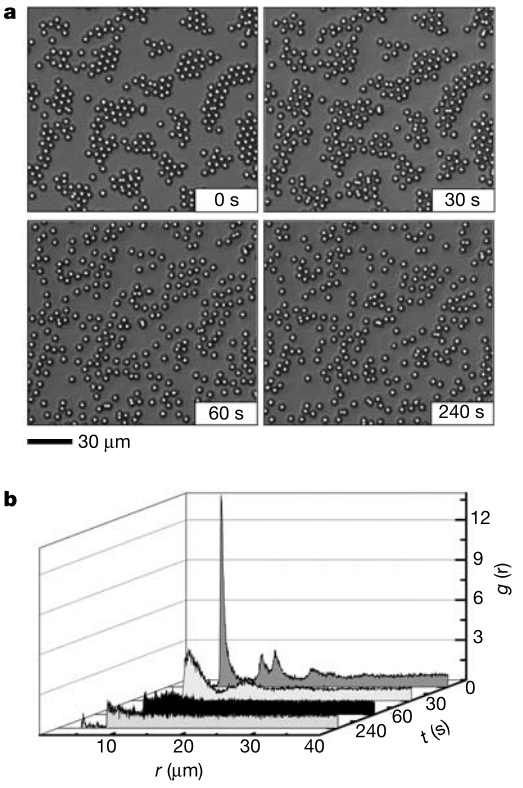

Figure 3 Protein-binding-triggered colloidal phase transition. **a**, Time sequence of images depicting the transition from a condensed to a dispersed colloidal phase, triggered by addition of protein (5 $\mu g\,ml^{-1}$ final concentration anti-Texas red rabbit monoclonal IgG antibody). Transitions were triggered only when the appropriate ligand was also incorporated into the membrane. **b**, Corresponding plots of $g(r)$ for the time sequence in **a**.

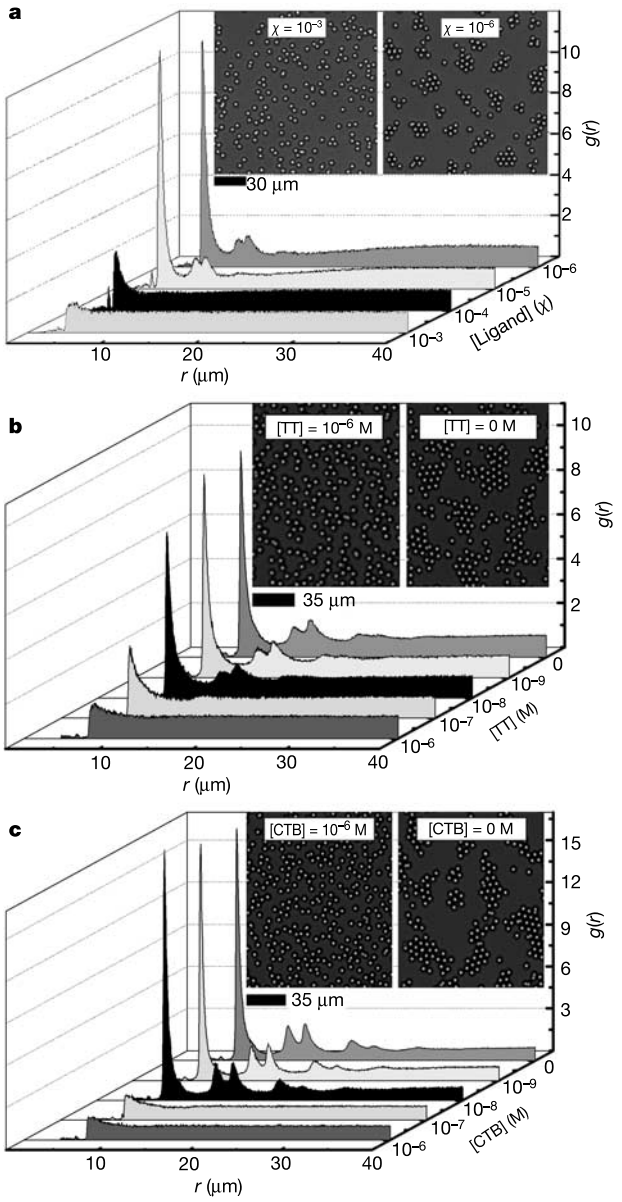

Figure 4 Protein-binding assays. **a**, Plots of measured $g(r)$ functions for dispersions of beads (area fraction $\phi = 0.15$) derivatized with fluid membranes (90% DMOPC, ~9% 1,2-dimyristoyl-*sn*-glycero-3-[phospho-L-serine] (DMPS)) containing different mole fractions (χ) of Texas red–DPPE ligand, after incubation with 20 $\mu g\,ml^{-1}$ anti-Texas red rabbit monoclonal IgG antibody. Dispersed phases formed for samples containing the membrane surface ligand at $\chi \geq 10^{-4}$. Inset images depict representative distributions, as labelled. **b**, Plots of $g(r)$ for a series of identical dispersions of 6.8-μm-diameter beads ($\phi = 0.25$) derivatized with membranes containing the ganglioside G_{T1B} (89.5% DMOPC, 9% DMPS, 0.5% G_{T1B}, 1% Texas red–DPPE), which have been incubated with various concentrations of TT. Binding of TT to membrane surface G_{T1B} induces a condensed-to-dispersed phase transition, as detected in the $g(r)$ plots as well as by direct observation of the colloid (inset images). **c**, Series of experiments as in **b**, except with 0.5% G_{M1} in place of G_{T1B}. Binding of CTB to the G_{M1} membrane surface induces the transition. Incubation of CTB with G_{T1B} colloids or TT with G_{M1} colloids produced no effect.

The protein systems studied here include antibody binding membrane surface antigen, and two different bacterial toxin proteins, cholera (CTB) and tetanus (TT), binding their respective membrane ligands, monosialoganglioside G_{M1} and trisialoganglioside G_{T1B}. Beads coated with 9% phosphatidylserine membranes formed condensed phases, consisting of short-lived crystallites, for all membrane surface ligands studied. In all cases, protein binding to membrane surfaces triggered a condensed-to-dispersed phase transition. Figure 3 depicts a time sequence of a phase transition triggered by addition of protein at time $t = 0$ s. These experiments were performed with ~300 μl of solution in ~5-mm round wells of a 96-well plate. Within 30 s of adding a drop of protein solution to the top of the well, uniform disruption of the condensed phase was discernible. Within 60 s, the colloid attained a dispersed distribution. Individual bead mobility is unaffected by protein binding. Exposure to a particular protein of interest triggered a phase transition only when the appropriate cognate ligand was incorporated into the colloid membrane. The physical presence of protein bound to the membrane surface increases the closest approach position between two membranes[15] and, correspondingly, reduces the cumulative strength of the van der Waals attraction between beads.

Quantitative analysis of the colloidal phases was performed by extracting the pair distribution function, $g(r)$. Bead positions were measured from wide-field (~1 mm^2) images by an object-locating algorithm to a precision of ~16 nm. Experiments were generally carried out at bead area fractions of $\phi \approx 0.15$–0.25, corresponding to ~7,000 individual beads per image. 5–10 independent images were averaged to generate $g(r)$ from $>10^8$ measured pair distances. For a finite rectangular window of spatial dimensions X by Y, $g(r)$ can be computed from

$$g(r) = \frac{\eta(r)X^2Y^2}{N(N-1)\delta r[\pi XYr - 2(X+Y)r^2 + r^3]} \qquad (1)$$

where $\eta(r)$ is the number of bead pairs with separation distance $r \pm \delta r/2$ ($\delta r = 40$ nm for the data presented here) and N is the total number of beads (see Supplementary Information).

Plots of $g(r)$ for different time points during a phase transition triggered by protein binding are illustrated in Fig. 3b. The condensed phase $g(r)$ is characterized by a large peak at the nearest-neighbour separation distance of one bead diameter (r_0), and secondary peaks occurring at $r = \sqrt{3}r_0$ and $2r_0$, corresponding to next-nearest neighbours in the hexagonal crystallites. Independent measurements of $g(r)$ were highly consistent. Standard deviations in the magnitude of the r_0 peak determined from separate colloidal preparations were generally less than 5%. Dispersed phases, consisting of random distributions and correspondingly flat $g(r)$ functions, are visibly distinguishable from condensed phases. Quantitative determination of $g(r)$ additionally distinguishes a range of intermediate distributions. These can be transient, such as the dispersing crystallites in Fig. 3a, $t = 30$ s. Intermediate degrees of order were also observed in near-equilibrium distributions, corresponding to differing amounts of protein binding on the membrane surface.

Measurements of near-equilibrium colloidal distributions over a range of protein and ligand concentrations were performed to explore the utility of the phase transition as a readout of protein binding on membrane surfaces. Antibody studies were performed using a monoclonal IgG antibody that binds the fluorescent membrane probe, Texas red–DPPE. Samples incubated with 20 μg ml^{-1} anti-Texas red antibody exhibit a clear transition from condensed to dispersed phases for ligand surface concentrations $\geq 10^{-4}$ monolayer (Fig. 4a). This corresponds to about ten ligand molecules on each membrane within the contact region where intermembrane separations are <10 nm (5-μm beads). For bacterial toxin binding studies, the ganglioside ligands G_{T1B} or G_{M1} were incorporated into membranes at a constant 0.5%. Incubation with TT triggered formation of a dispersed phase in the G_{T1B}-containing colloid, while no effect was produced in the G_{M1} colloid (Fig. 4b). Analogously, exposure to CTB triggered the transition to a dispersed phase in the G_{M1} colloid without producing any effect on the G_{T1B} colloid (Fig. 4c). Exposure to bungarotoxin (1 μM) produced no effect in either colloid. In a parallel set of experiments on planar supported membranes, the effective dissociation constants for TT–G_{T1B} and CTB–G_{M1} binding under these conditions were directly measured to be ~60 and ~41 nM, respectively (see Supplementary Information). The magnitude of the r_0 peak in the measured $g(r)$ traces the surface concentration of bound protein.

The membrane-derivatized colloidal system introduced here has potential applications to a broad set of problems involving chemical events on cell membrane surfaces. These range from mapping ligand interactions with numerous cell surface proteins to detection of membrane-targeting bacterial toxins (for example, botulism, cholera, anthrax, tetanus) and viruses. Membrane-derivatized beads can be combined in heterogeneous mixtures or with live cells (for example, rosetting), allowing the methodology outlined here to be applied to analysis of intermembrane receptor–ligand interactions. Implementation of the colloid assay is amenable to automated liquid handling and imaging systems. Detailed analysis of spatial distribution functions, such as the pair distribution studied here, enables characterization of subtle interactions, including those that may not produce qualitatively recognizable effects. At the same time, the use of membrane coatings on colloidal particles offers an extensive repertoire of chemical functionality, which may prove valuable in non-biological settings. We anticipate that the general principles illustrated with lipid membranes in this work could be extended to other materials, such as the recently developed polymer vesicles[16]. □

Received 24 July; accepted 14 November 2003; doi:10.1038/nature02209.

1. Sackmann, E. Supported membranes: Scientific and practical applications. *Science* **271,** 43–48 (1996).
2. Groves, J. T. Membrane array technology for drug discovery. *Curr. Opin. Drug Discov. Dev.* **5,** 606–612 (2002).
3. Grakoui, A. *et al.* The immunological synapse: A molecular machine controlling T cell activation. *Science* **285,** 221–227 (1999).
4. Fang, Y., Frutos, A. G. & Lahiri, J. Membrane protein microarrays. *J. Am. Chem. Soc.* **124,** 2394–2395 (2002).
5. Hoffman, T. L., Canziani, G., Jia, L., Rucker, J. & Doms, R. W. A biosensor assay for studying ligand-membrane receptor interactions: binding of antibodies and HIV-1 Env to chemokine receptors. *Proc. Natl Acad. Sci. USA* **97,** 11215–11220 (2000).
6. Yang, T., Jung, S.-y., Mao, H. & Cremer, P. S. Fabrication of phospholipid bilayer-coated microchannels for on-chip immunoassays. *Anal. Chem.* **73,** 165–169 (2001).
7. Anderson, V. J. & Lekkerkerker, H. N. W. Insights into phase transition kinetics from colloid science. *Nature* **416,** 811–815 (2002).
8. Yethiraj, A. & van Blaaderen, A. A colloidal model system with an interaction tunable from hard sphere to soft and dipolar. *Nature* **421,** 513–517 (2003).
9. Ramos, L., Lubensky, T. C., Dan, N., Nelson, P. & Weitz, D. A. Surfactant-mediated two-dimensional crystallization of colloidal crystals. *Science* **286,** 2325–2328 (1999).
10. Dinsmore, A. D. *et al.* Colloidosomes: selectively permeable capsules composed of colloidal particles. *Science* **298,** 1006–1009 (2002).
11. Manoharan, V. N., Elsesser, M. T. & Pine, D. J. Dense packing and symmetry in small clusters of microspheres. *Science* **301,** 483–487 (2003).
12. Yang, P. *et al.* Hierarchically ordered oxides. *Science* **282,** 2244–2246 (1998).
13. Bayerl, T. M. & Bloom, M. Physical properties of single phospholipid bilayers adsorbed to micro glass beads. *Biophys. J.* **58,** 357–362 (1990).
14. Buranda, T. *et al.* Biomimetic molecular assemblies on glass and mesoporous silica microbeads for biotechnology. *Langmuir* **19,** 1654–1663 (2003).
15. Wong, A. P. & Groves, J. T. Molecular topography imaging by intermembrane fluorescence resonance energy transfer. *Proc. Natl Acad. Sci. USA* **99,** 14147–14152 (2002).
16. Discher, D. E. & Eisenberg, A. Polymer vesicles. *Science* **297,** 967–973 (2002).

Supplementary Information accompanies the paper on **www.nature.com/nature**.

Acknowledgements We thank R. Parthasarathy and N. Clack for discussions, and D. Discher for advice on the manuscript. M.J. was supported by a Fulbright scholarship and by the Czech Republic Ministry of Education. This work was supported in part by the Burroughs Wellcome Career Award in the Biomedical Sciences (to J.T.G.) and by the US Department of Energy.

Competing interests statement The authors declare that they have no competing financial interests.

Correspondence and requests for materials should be addressed to J.T.G. (JTGroves@lbl.gov).